

Time-dependent treatment of two-photon resonant single and double ionization of helium by ultrashort laser pulses

A. Palacios,¹ T. N. Rescigno,¹ and C. W. McCurdy^{1,2}

¹*Chemical Sciences, Lawrence Berkeley National Laboratory, Berkeley, California 94720, USA*

²*Departments of Applied Science and Chemistry, University of California–Davis, Davis, California 95616, USA*

(Received 31 December 2008; published 5 March 2009)

We report the results of accurate time-dependent calculations of two-photon ionization of helium by ultrashort pulses. Ionization amplitudes and generalized cross sections are extracted from the wave function using exterior complex scaling. For photon energies above the first ionization threshold, two-photon single ionization is enhanced by core excited resonances, in processes visible with pulses as short as 2 fs, when the photon frequency is equal to a transition energy in He⁺. We explore the dependence of the total cross section in the vicinity of the threshold for sequential double ionization on pulse duration. A signature in the single differential cross section of two-photon sequential ionization with the ground state of the ion as the intermediate state is seen to be suppressed by sufficiently short pulses in favor of the nonsequential process, while the triple differential cross section shows that attosecond pulses can access different electron dynamics than those of longer duration. The peaks in the single differential cross section due to sequential ionization with the excited intermediate states of the ion are observed to occur at energies displaced by about 2 eV from the expected values by interference effects between continuum channels.

DOI: [10.1103/PhysRevA.79.033402](https://doi.org/10.1103/PhysRevA.79.033402)

PACS number(s): 32.80.Fb, 32.80.Rm

I. INTRODUCTION

In recent years, with the advent of high harmonic generation of subfemtosecond pulses in the ultraviolet and soft x-ray regions [1] and the prospect that free-electron lasers may provide more intense pulses of similarly short duration, interest has increasingly focused on the initial benchmark experiments that will demonstrate the capabilities of intense ultrashort radiation pulses to probe electron dynamics. Some experiments that explore the effects of electron correlation in atoms and molecules on these time scales are already being performed [2–4] and their results have underscored the necessity for reliable theoretical calculations for their interpretation and for designing subsequent experiments.

To that end, theoretical and numerical methods that provide essentially exact solutions of the time-dependent Schrödinger equation for two-electron systems subject to short pulses have increasingly been the subject of theoretical work in this emerging field [5–12]. Because a central goal of these theoretical efforts is the accurate and detailed prediction of the results of pump-probe experiments combining ultrashort extreme ultraviolet with infrared or x-ray pulse, the unambiguous analysis of the wave function following a single short pulse or sequence of pulses is critical for such studies. We have recently demonstrated how numerical methods based on exterior complex scaling (ECS) of the electronic coordinates can accomplish that analysis in systems with two active electrons [13,14]. Our approach uses a combination of finite-element method with a discrete variable representation (FEM-DVR) [15] to provide an efficient procedure for time propagation and analysis of the wave function.

In this study we apply these methods to the study of several aspects of two-photon single and double ionization of helium by ultrashort pulses. We focus on how finite-length pulses can modify and sometimes obscure those processes

while in principle establishing their natural time scales.

At photon energies greater than the first ionization energy of helium, where above threshold ionization (ATI) of the atom can produce He⁺ in its ground or excited states, Shakeshaft and co-workers [16,17] explained with time-independent studies why enhancement should occur at “core excited resonances” where the photon energy coincides with a transition energy in the ion. For example, above the threshold to produce He⁺ in its $n=2$ levels, a peak in the cross section for two-photon single ionization to produce the ion excited to its $2p$ level should occur when the photon energy is equal to the $1s$ to $2p$ transition energy in He⁺. We show how this process appears in the cross section extracted from pulses of duration up to 2 fs and how the entire series of such resonances is contained in the resulting electronic wave packets as the central frequency is raised.

In two-photon double ionization, the cross section can rise dramatically [18–21] as the photon energy approaches the threshold for sequential ionization of an atom. Here we show how the apparent integral cross section for double ionization, extracted from ever longer pulses, behaves both immediately below and above that threshold. Below the threshold we see the same behavior seen by Feist *et al.* [21] in which the rise below threshold becomes sharper with longer pulses. Above that threshold we will demonstrate how the cross section begins to reflect the single-ionization cross sections of the helium atom and the helium cation.

Above the threshold for sequential ionization (54.4 eV) of helium the single differential cross section (SDCS) has two peaks corresponding to the energies of the sequentially ejected electrons superimposed on a background that includes ionization via the nonsequential process. As the pulse length is shortened we find that these peaks disappear and that the signature of sequential ionization seen for longer pulses in the angular dependence of the fully differential cross section (triple differential cross section or TDCS) is

suppressed. This behavior establishes an apparent time scale for the observation of the behaviors associated with the sequential ionization process. As the photon energy is raised above the second sequential threshold, beyond which the intermediate ionized state can be He^+ in its $2s$ or $2p$ state, four peaks appear in the SDCS, corresponding to the energies of the electrons ejected in the sequential processes with the first step leaving the ion in its ground or $n=2$ state. However, we find that the amplitudes for different sequential processes evidently interfere with one another for finite-length pulses, so that the second set of peaks appear shifted by as much as 2 eV.

In Sec. II we briefly describe the main points of the methods developed in two earlier publications and applied here. Section III describes our calculations revealing the pulse length dependence of features due to core excited resonances above threshold ionization. Our calculations on the behavior of double ionization between the first two sequential ionization thresholds with varying pulse durations are described in Sec. IV, and the interference phenomenon seen with ultrashort pulses above the second sequential threshold is discussed in Sec. V. We conclude with a summary of the pulse length effects we have observed and the evident time scales for the observation of the electron dynamics of ionization processes they suggest.

II. THEORY

The methods we apply in this study differ from other approaches that are also capable of producing essentially exact results for two-electron systems in two ways. First, we make use of ECS of the electronic coordinates to evaluate an expression in a single computational step that propagates the wave packet from the end of the radiation pulse to infinite time and simultaneously Fourier transforms it to produce a specific energy continuum wave function. Second, from those fixed-energy continuum functions we extract the amplitudes for ionization for a range of final-state energies within the bandwidth of the pulse using a surface integral formula involving the coordinates of both electrons.

Most of the formalism used here has been described in two previous papers [13,14], so we restrict ourselves in this section to a description of the main points and the working equations.

A. Amplitudes and cross sections for two-photon ionization

We begin with an atom initially in its ground state that is subjected to a radiation pulse that starts at $t=0$ and ends at $t=T$. The time evolution of the wave function along the pulse duration is obtained by numerically solving the time-dependent Schrödinger equation

$$i\frac{\partial}{\partial t}\Psi(t) = \mathcal{H}(t)\Psi(t), \quad (1)$$

where $\mathcal{H}(t) = H_0 + V_t$ with H_0 being the atomic Hamiltonian and V_t as the laser-atom interaction. In the dipole approximation, which is appropriate for the wavelengths we consider here, the laser-atom interaction in the length gauge is

given in terms of the dipole operator $\boldsymbol{\mu} = -e\sum_i \mathbf{r}_i$ and the electric field $\mathbf{E}(t)$ by $V_t = \mathbf{E}(t) \cdot \boldsymbol{\mu}$. The calculations we present here were performed in the length gauge, although we used the velocity gauge for convergence tests. For a photon energy ω and a total pulse duration T , $\mathbf{E}(t)$ may be written as

$$\mathbf{E}(t) = \begin{cases} E_0 F_\omega(t) \hat{\boldsymbol{\epsilon}}, & t \in [0, T], \\ 0, & \text{elsewhere,} \end{cases} \quad (2)$$

where E_0 is the maximum field strength and $\hat{\boldsymbol{\epsilon}}$ is the polarization vector. We choose a sine-squared envelope for the time dependence of the pulse, $F_\omega(t)$,

$$F_\omega(t) = \sin^2\left(\frac{\pi}{T}t\right) \sin(\omega t). \quad (3)$$

Once the pulse has finished at $t=T$ the outgoing electrons are still interacting with each other and the nucleus and for $t > T$ the wave packet describing the system propagates under the influence of the atomic Hamiltonian H_0 . Following the arguments in Refs. [13,14] we define a scattered wave corresponding to a specific final total energy E as the Fourier transform of the time propagated packet

$$\Psi_{\text{sc}} \equiv -i \lim_{\gamma \rightarrow 0} \int_0^\infty dt e^{i(E+i\gamma-H_0)t} \Psi(T) \quad (4)$$

and note that Ψ_{sc} , from which all the physical information will be extracted, satisfies the time-independent-driven equation

$$(E - H)\Psi_{\text{sc}} = \Psi(T) \quad (5)$$

with pure outgoing boundary conditions. It is in the solution of Eq. (5) that we apply the ECS transformation in which the electronic coordinates are scaled only beyond a radius R_0 by a complex phase factor according to $r \rightarrow R_0 + (r - R_0)e^{i\eta}$. The value of R_0 is chosen large enough that the wave packet can be assumed not to have reached that radius during the pulse. As is now well established [22], solving Eq. (5) with the boundary condition that the solution vanishes at the end of the complex portion of the numerical grid on which it is represented is formally equivalent to applying outgoing boundary conditions, no matter how many electrons are being ejected.

To see how the amplitudes for single and double ionization can be extracted from Ψ_{sc} we note that the wave packet at the end of the pulse can be formally expanded as

$$\begin{aligned} \Psi(\mathbf{r}_1, \mathbf{r}_2, T) &= \psi_{\text{bound}}(\mathbf{r}_1, \mathbf{r}_2) + \psi_{\text{single}}(\mathbf{r}_1, \mathbf{r}_2) + \psi_{\text{double}}(\mathbf{r}_1, \mathbf{r}_2) \\ &= \psi_{\text{bound}}(\mathbf{r}_1, \mathbf{r}_2) + \sum_n \int dk_n^3 C(\mathbf{k}_n) \psi_{\mathbf{k}_n}^-(\mathbf{r}_1, \mathbf{r}_2) \\ &\quad + \int dk_1^3 \int dk_2^3 C(\mathbf{k}_1, \mathbf{k}_2) \psi_{\mathbf{k}_1, \mathbf{k}_2}^-(\mathbf{r}_1, \mathbf{r}_2), \end{aligned} \quad (6)$$

where $\psi_{\text{bound}}(\mathbf{r}_1, \mathbf{r}_2)$ contains the contributions from the bound states of the target, n runs over the bound states of He^+ , and the coefficients $C(\mathbf{k}_n)$ and $C(\mathbf{k}_1, \mathbf{k}_2)$ are amplitudes for single and double ionization, respectively.

It can be shown [13,14] that these amplitudes are contained in the asymptotic behavior of Ψ_{sc} for the total energy

E in Eq. (5) corresponding to the final-state momenta \mathbf{k}_n or \mathbf{k}_1 and \mathbf{k}_2 . For an atomic target they can be extracted using surface integrals involving Ψ_{sc} and atomic Coulomb functions [22]. For single ionization the amplitude is given by

$$C(\mathbf{k}_n) = \frac{1}{2} \int \{ \phi_{\mathbf{k}}^{-*}(\mathbf{r}_1) \psi_n^*(\mathbf{r}_2) [\nabla \Psi_{sc}(\mathbf{r}_1, \mathbf{r}_2)] - \Psi_{sc}(\mathbf{r}_1, \mathbf{r}_2) \nabla [\phi_{\mathbf{k}}^{-*}(\mathbf{r}_1) \psi_n^*(\mathbf{r}_2)] \} \cdot d\mathbf{S}, \quad (7)$$

while for double ionization we have

$$C(\mathbf{k}_1, \mathbf{k}_2) = \frac{1}{2} e^{i\chi} \int \{ \phi_{\mathbf{k}_1}^{-*}(\mathbf{r}_1) \phi_{\mathbf{k}_2}^{-*}(\mathbf{r}_2) \nabla \Psi_{sc}(\mathbf{r}_1, \mathbf{r}_2) - \Psi_{sc}(\mathbf{r}_1, \mathbf{r}_2) \nabla [\phi_{\mathbf{k}_1}^{-*}(\mathbf{r}_1) \phi_{\mathbf{k}_2}^{-*}(\mathbf{r}_2)] \} \cdot d\mathbf{S}, \quad (8)$$

where the two-electron gradient is $\nabla = (\nabla_1, \nabla_2)$, $\psi_n(\mathbf{r}_2)$ are the bound states of He^+ , and the testing functions $\phi_{\mathbf{k}}^-$ are momentum-normalized Coulomb functions with a nuclear charge $Z=1$ for single ionization and $Z=2$ for double ionization. We emphasize that these are not approximations to the final state of the system, but instead are the appropriate functions to extract the asymptotic amplitudes from Ψ_{sc} in the limit of a large volume enclosed by the surface integral, as can be shown from stationary phase arguments. In the formula for the double-ionization amplitudes, χ is an irrelevant

volume-dependent overall phase that makes no contribution to any physical observable [22].

The single- and double-ionization amplitudes $C(\mathbf{k}_n)$ and $C(\mathbf{k}_1, \mathbf{k}_2)$ are the amplitudes specific to a particular radiation pulse. If the fields involved are such that the physics of photoejection can be treated with first- or second-order time-dependent perturbation theory, we can take advantage of the fact that they can be computed over a range of energies within the bandwidth of the pulse to extract the (generalized) cross sections for single and double ionization over that range from the solution of the time-dependent Schrödinger equation for a single pulse. The derivation [13,14] of the working equations is lengthy and will not be reproduced here; they are

$$\frac{d\sigma^{2\omega}}{d\Omega} = \frac{8\pi^3 \hbar^3 (\Delta E_{fi}/2)^2 m k_n}{c^2 |E_0|^4} \frac{|C(\mathbf{k}_n)|^2}{|\tilde{\mathfrak{F}}(E_f, E_i, \omega, T)|^2} \quad (9)$$

for single ionization and

$$\frac{d\sigma^{2\omega}}{dE_1 d\Omega_1 d\Omega_2} = \frac{8\pi^3 (\Delta E_{fi}/2)^2 m^2 \hbar k_1 k_2}{c^2 |E_0|^4} \frac{|C(\mathbf{k}_1, \mathbf{k}_2)|^2}{|\tilde{\mathfrak{F}}(E_f, E_i, \omega, T)|^2} \quad (10)$$

for double ionization. In these equations the effective energy shape function for the radiation pulse is given by

$$\tilde{\mathfrak{F}}(E_f, E_i, \omega, T) = \frac{6e^{-iT(2\omega - \Delta E_{fi})} (-1 + e^{iT(2\omega - \Delta E_{fi})}) \pi^4}{(2\omega - \Delta E_{fi}) [T^4 (2\omega - \Delta E_{fi})^4 - 20\pi^2 T^2 (2\omega - \Delta E_{fi})^2 + 64\pi^4]}, \quad (11)$$

where E_i is the energy of the initial state and E_f is the energy of the final state, $k_1^2/2 + k_2^2/2$ for double ionization and the sum of $k_n^2/2$ and the energy of He^+ state n in the case of single ionization, and $\Delta E_{fi} = E_f - E_i$.

While it is a significant computational advantage to be able to extract the cross section over a range of energies contained in a single radiation pulse, it is formally only possible to do so in the case of two-photon ionization in the limit of long pulses if there are sharp features due to intermediate-state resonances. For finite-length pulses these formulas give the apparent cross section in which sharp resonant features appear as they would if the apparent cross section had been defined in terms of the rate of ionization divided by the square of the field intensity, as is done in other well-established computational approaches [21,23–25].

Thus the results we present here reflect the competition of various resonant and nonresonant processes during the radiation pulse. As we have demonstrated previously, these results are not limited by the overall time interval during which the time-dependent Schrödinger equation was solved, because the solution of Eq. (5) implies an infinite propagation interval. We have shown that closely spaced autoionizing double excited states of He can be resolved using these methods when excited by a 900 as pulse [14]. Consequently the de-

pendence of the apparent cross sections on pulse duration establishes an evident physical time scale for the completion of the processes that contribute to them.

B. Numerical implementation

We represent the wave function in terms of products of two-electron radial functions and coupled spherical harmonics,

$$\Psi(\mathbf{r}_1, \mathbf{r}_2, t) = \sum_{l_1, l_2, L}^{l_{\max}, L_{\max}} \psi_{l_1, l_2, L}(r_1, r_2, t) \mathcal{Y}_{l_1, l_2}^{L, M=0}(\mathbf{r}_1, \mathbf{r}_2), \quad (12)$$

including all (L, l_1, l_2) configurations that can be constructed using some given value of l_{\max} for the individual electron angular momenta and L_{\max} for the total orbital angular momentum. Our calculations here are restricted to weak fields and convergence is achieved by including only $L=0, 1, 2$, as we have verified by carrying out calculations at these field intensities with $L_{\max}=3$. On the other hand, the convergence of the sums over l_1 and l_2 must be tested for each quantity we calculate. As we will show in the following discussion, converged results for total cross sections can be achieved by using $l_{\max}=3$, whereas the l_{\max} value required to converge the

triple differential cross sections will depend on the photon energy and reflects the dominance of the sequential or non-sequential process in the case of double ionization.

The radial degrees of freedom are discretized using a FEM-DVR with a product basis of Lobatto shape functions [15,22]. The time propagation in the presence of the field is carried out by using a Crank-Nicholson propagator (see details in Ref. [13]) on the real part of the FEM-DVR grid. The end of the real part of the grid, R_0 , must be chosen large enough to contain the spreading wave packet over the duration of the pulse and avoid unphysical reflections from the grid boundaries. Once the pulse is over, the resulting wave packet is taken as the driving term for the scattered wave equation, which is solved with a complex portion extending beyond R_0 by 50 or 60 bohr. We emphasize that given the parameters of a particular pulse, the time propagation is carried out only once and then the scattered wave equation can be solved for any energy within the pulse bandwidth.

Unless otherwise noted, all the results shown here have been obtained for an intensity $I=10^{12}$ W cm $^{-2}$, which is high enough to provide relatively large ionization rates for one- and two-photon transitions and low enough to avoid higher nonlinear processes from taking place, thereby allowing comparison with previous calculations carried out using time-dependent perturbation theory. At these intensities, therefore, dipole selection rules imply that the only accessible states are those with symmetries $^1S^e$, $^1P^o$, and $^1D^e$.

The ground-state wave function Ψ_0 , which forms the initial wave packet, was obtained by diagonalizing the field-free Hamiltonian on a portion of the real grid with a maximum r of ≈ 50 bohr, with configurations representing total angular momentum $L=0$ and the same value of l_{\max} that was used in the subsequent time propagation.

III. TWO-PHOTON SINGLE IONIZATION IN THE ATI REGION

The ATI region begins at a photon energy equal to the ionization threshold of 24.59 eV. In Fig. 1 we show the calculated total cross section for single ionization

$$\sigma_{\text{tot}} = \sum_n^{\text{open}} \int d\Omega \frac{d\sigma_n^{2\omega}}{d\Omega} \quad (13)$$

in which the contributions from all open channels have been included at each photon energy. At photon energies below 39.51 eV only single ionization can occur and we see a sequence of $^1S^e$ and $^1D^e$ autoionizing states of He appearing in the calculated cross section which we have also seen in earlier calculations [14]. Their excitation is resolved in these calculations because the effective propagation of the wave packet to infinite time after the pulse via Eq. (5) allows the analysis of the final state with arbitrary resolution. The autoionizing states excited by the pulse are therefore allowed to decay with their correct decay widths and display their true Fano profiles.

Above that threshold for double ionization at a photon energy of 39.51 eV single and double photoionization compete, but the amplitudes for the two processes are disen-

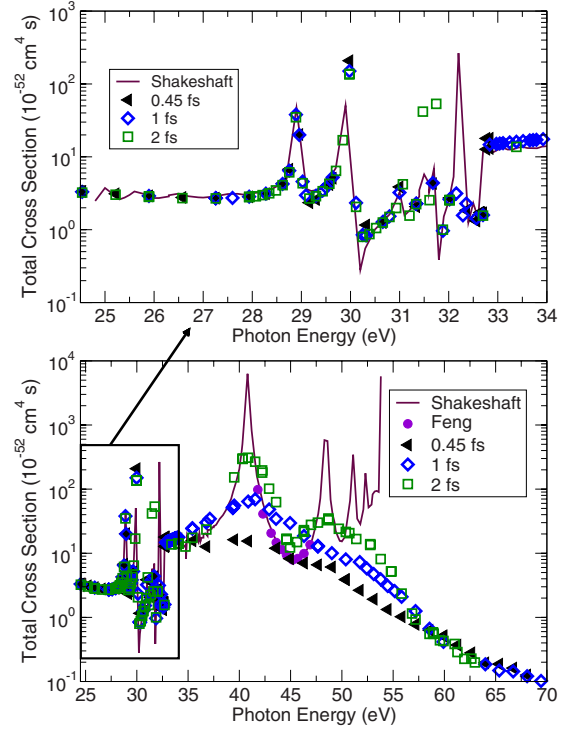


FIG. 1. (Color online) Two-photon single-ionization total cross sections as a function of photon energy. Present results: triangles (0.45 fs), diamonds (1 fs), and squares (2 fs). Full line: Ref. [17]. Circles: Ref. [26].

tangled by the surface integrals in Eqs. (7) and (8) that extract them from the wave packet. The features seen in the total single-ionization cross section at these energies are due to core excited resonances discussed by Shakeshaft and co-workers [16,17]. We show results at three pulse durations, but only for pulse durations greater than about 1 fs are these peaks visible.

The resonances are predicted in second-order perturbation theory to appear in the partial cross section for excitation ionization leaving the He $^+$ ion in its excited state with quantum numbers n, l at photon energies equal to transition energies from lower states of the ion to that final state, i.e.,

$$\hbar\omega = E_{n,l}^{\text{ion}} - E_{n',l'}^{\text{ion}}, \quad (14)$$

where $n > n'$. These resonances come from the contribution to the sum and integral over intermediate states in perturbation theory of excited ionized states of He $^+$ paired with an outgoing electron with momentum equal to that of the final momentum in the two-photon ionization process. Shakeshaft points out that in second-order perturbation theory, unlike the peaks due to resonances associated with the excitation of bound intermediate states, these are not singularities in the cross section, but are “smoothed out” by the integral over intermediate continuum states in the perturbation-theory expression. The results of time-independent calculations by Shakeshaft and Feng and van der Hart [26] are also shown in Fig. 1, and the former show a sharp series of resonances in contrast to the present time-dependent results for the total cross section.

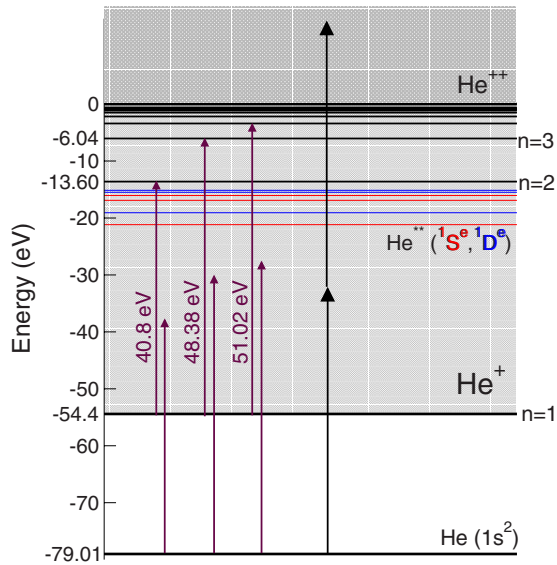


FIG. 2. (Color online) Schematic representation of the two-photon single-ionization process showing the photon energies at which core excited resonances are predicted to occur.

In Fig. 2 we show the energies at which these resonances should occur to emphasize that there is an infinite series of them associated with excitation of higher states of the ion, each appearing at a photon energy above that where the corresponding excitation ionization channel has opened. At the resonant energy, the final energy of the electron corresponds to that of the sequential process in which the first photon ionizes the atom leaving it in its ground state, while the second photon excites the ion.

In Fig. 3 we show the contribution of the partial cross sections for excitation ionization leading to excited states of the ion extracted from pulses of various durations. In this comparison, above the clearly visible thresholds for these channels, we see more clearly the appearance of the sequence of core excited resonances at a pulse duration between 0.5 and 1 fs. The dependence on pulse duration is seen for excitation ionization up through the $n=5$ threshold, and the peak maxima match the resonance energies in Eq. (14). This comparison establishes an apparent time scale for observing the resonance process that leads to those peaks. Although their calculations did not involve finite-length pulses, Proulx *et al.* [16] speculated in the original paper on this subject, which treated photodetachment of the hydrogen anion, that the coherence time of the light, and therefore the pulse duration, would have to be longer than all other relevant time scales, including that of electron correlation, in order for their time-independent calculation producing those resonance peaks to be valid. This calculation evidently establishes that time scale.

In the bottom panel of Fig. 3, structures begin to appear in the partial cross sections for a pulse duration of 2 fs that arise from the $^1P^o$ doubly excited states of helium that can be populated by one-photon absorption and play the role of intermediate-state resonances. The peaks in the $2s$ and $2p$ partial cross sections for excitation ionization in that panel correspond to the $^1P^o$ ($2s2p$) state known [27] to lie at

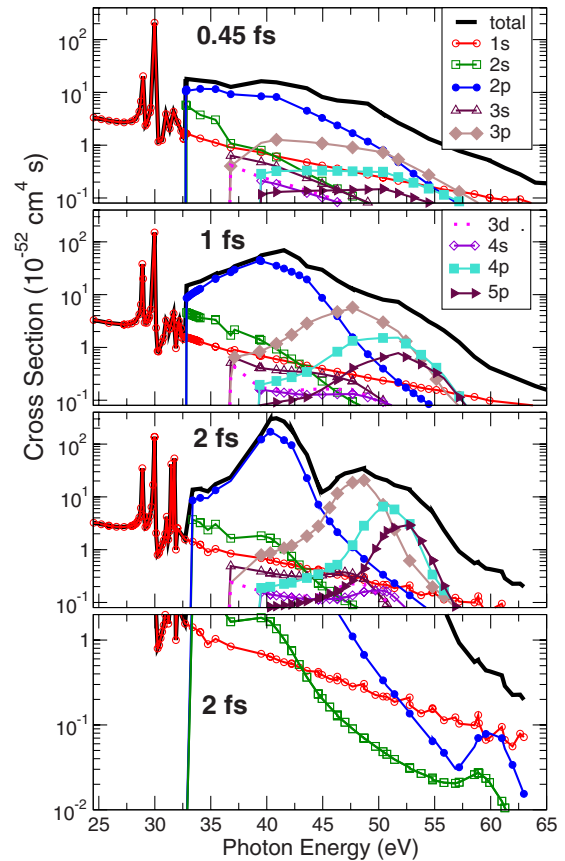


FIG. 3. (Color online) Contributions of the partial cross sections for excitation ionization leading to different states of He^+ to the total two-photon single-ionization cross section.

60.145 eV with a lifetime of approximately 16 fs. Of course at a pulse length of 2 fs these features are poorly resolved.

IV. TWO-PHOTON DOUBLE IONIZATION

The threshold for two-photon double ionization is 39.5 eV and the amplitudes for that process are contained in the same wave packets from which the amplitudes for single ionization and excitation ionization described in Sec. III are extracted. In Fig. 4 we show the total cross section for double ionization, calculated for various pulse durations, below the threshold for the sequential process at 54.4 eV, as well as the apparent total cross section above that threshold extracted from the wave packets using Eq. (10) and integrating over the angular dependence and energy sharing. In that figure we compare our results below the sequential threshold with the only two experimental data points available [28,29], as well as with the results of time-independent calculations by Horner *et al.* [18] and the finite pulse calculations of Feist *et al.* [21]. Horner *et al.* predicted the rapid rise of the total cross section below the double-ionization threshold, pointing out that it is due to the virtual contribution of the singly ionized intermediate states associated with the energetically closed sequential ionization process, and that behavior was later confirmed by Feist *et al.* [21]. In the present calculations we find essentially perfect agreement with Feist *et al.* below 53

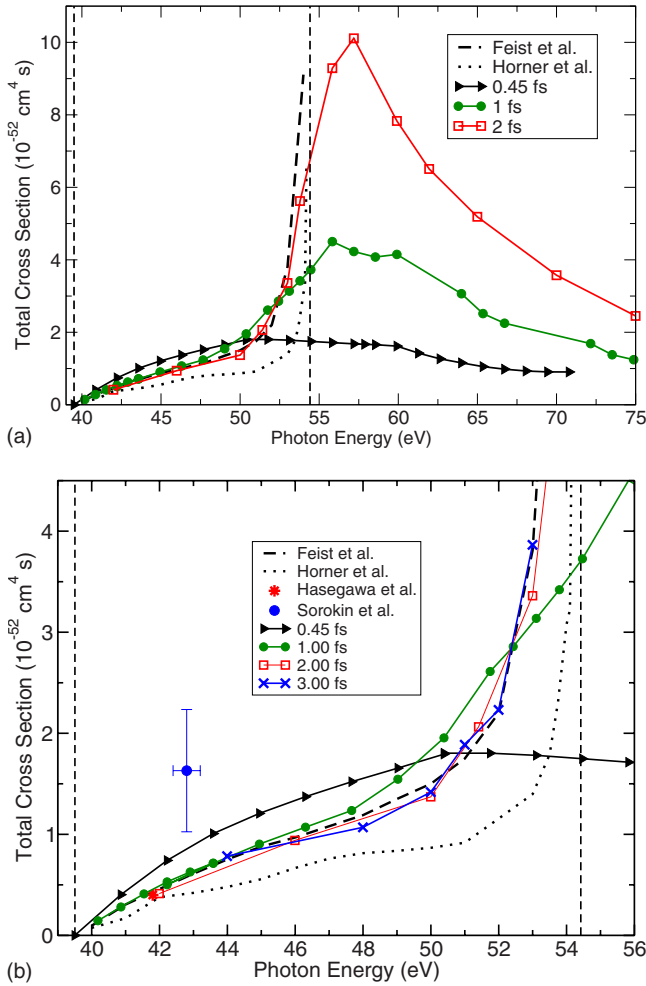


FIG. 4. (Color online) Total two-photon double-ionization cross sections as a function of photon energy. The current results are labeled with the corresponding pulse durations.

eV when 3 fs pulses are used. The entire range of data plotted in this figure was computed by propagating only seven pulses and extracting the cross section within their bandwidths using Eq. (10).

That procedure can also be used above the sequential threshold to calculate an apparent total cross section, but that apparent cross section will continue to increase with pulse duration. Nonetheless its shape can be understood by referring to the simple model for the contribution of sequential ionization to the SDCS described in the Appendix. When plotted as a function of the energy of either ejected electron, the SDCS shows two peaks, one at $E_1 = E_i - \epsilon_{1s} + \hbar\omega$ and the other $E_1 = \epsilon_{1s} + \hbar\omega$, where the orbital energy of the He^+ ion, ϵ_{1s} , and the energy of the ground state of He, E_i , are negative and referenced to the zero of energy of the three separated particles. According to Eq. (A11) the heights of those peaks are controlled by the pulse duration and the product of the single-ionization cross sections $\sigma^{\text{He}}(E_i - \epsilon_{1s} + \hbar\omega)\sigma^{\text{He}^+}(\epsilon_{1s} + \hbar\omega)$. Therefore once the pulse duration T is large enough to make two well-resolved peaks in the SDCS, the integral of the SDCS extracted from such pulses for various photon energies produces a curve like that shown for 2 fs in the upper panel of Fig. 4, which falls off with ω above the sequential

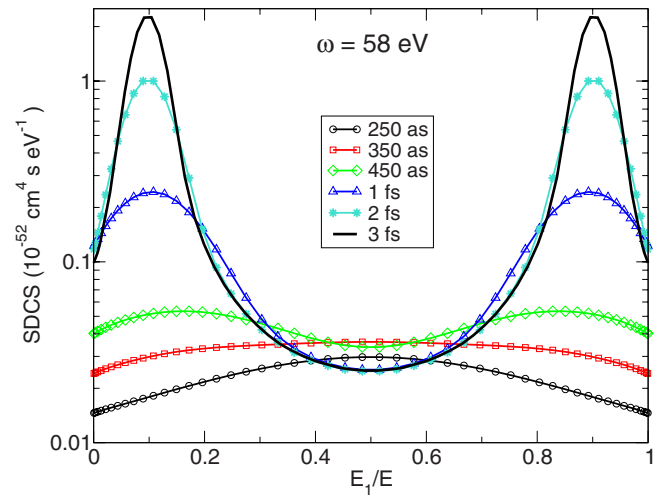


FIG. 5. (Color online) Single differential cross sections for a photon energy (58 eV) above the sequential ionization threshold for two-photon double ionization obtained with different pulse durations.

threshold like the product of the two single-ionization cross sections.

An example of the behavior of the corresponding SDCS with varying pulse durations is shown in Fig. 5. For 3 fs pulses we find two distinct peaks in the SDCS which broaden and disappear as the pulse is shortened to 250 as. It might be tempting to conclude, based on the behavior of the SDCS alone, that the sequential process has been at least partially extinguished in favor of the nonsequential process for subfemtosecond pulses. However, as we show in the Appendix, it is possible to make an approximation to the SDCS that reproduces the behavior of Fig. 5 within 10%–15% using time-dependent perturbation theory, yet neglects correlation and screening entirely. The results of that approximation is shown in Fig. 13 in the Appendix for comparison. Thus, to see whether different electron dynamics are being probed by subfemtosecond pulses from that being revealed by longer pulses, we need to focus on a more detailed quantity, namely, the TDCS.

First we need to establish the qualitative behavior of the TDCS for longer pulses, so in Fig. 6 we plot the TDCS both at a photon energy of 46 eV, below the sequential threshold, and at 58 eV, above the threshold, for a pulse duration of 1 fs. In that figure we see the general trends pointed out by Horner *et al.* [20] in time-independent calculations and also by Feist *et al.* [21] in calculations using finite pulses. At 46 eV where only nonsequential ionization can occur we see that the two electrons are ejected predominantly in a back-to-back geometry except for ejection directions approaching perpendicular to the polarization vector. We show the TDCS for equal-energy sharing in that case, but the cross sections are similar for all but the most extreme energy sharings. The TDCS is smaller by about a factor 40 when either electron is detected perpendicular to the polarization direction. That behavior is reminiscent of the TDCS in the sequential region where it is approximately described by product of dipole patterns, in this case $\cos^2(\theta_1)\cos^2(\theta_2)$, as can be seen in Fig. 6 in the TDCS at 58 eV plotted for an energy sharing corre-

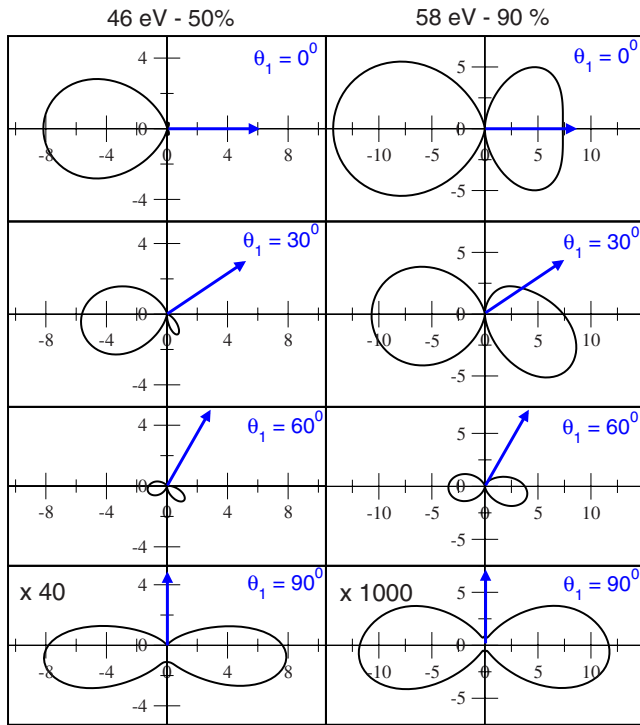


FIG. 6. (Color online) TDCS at 46 with 50% energy sharing (left column) and 58 eV with 90% energy sharing (right column). Each row corresponds to a different angle of one electron fixed with respect to the polarization vector (horizontal axis). Results are shown for a pulse duration of 1 fs and calculated with $l_{\max}=7$.

sponding to one of the sequential peaks in Fig. 5. In this case we see a mostly uncorrelated angular behavior in which the angular distribution for any direction of the electron plotted by the arrow is approximately proportional to $\cos^2(\theta_1)$ and nearly extinguishes when one electron is ejected perpendicular to the polarization direction.

In Fig. 7 we show the TDCS as function of energy sharings for pulse durations of 1 and 3 fs at 52 eV, just below the sequential threshold, and above the threshold at 58 eV. In all cases one electron goes out along the polarization direction. In the left column of that figure, where the results just below the sequential threshold are plotted, we see the rise in the magnitude of the TDCS at extreme energy sharings and the beginning of the angular behavior that becomes the signature of sequential ionization shown in the right column at 58 eV. In that column we see the sequential peaks sharpening toward the characteristic $\cos^2(\theta)$ behavior at the sequential energies shown in the time-independent calculations in the bottom row as the pulse duration is increased.

With these observations about the TDCS for longer pulses, we are in a position to analyze the TDCS in the sequential region for subfemtosecond pulses. In Fig. 8 we compare the angular dependences of ejection by 1 fs, 450 as, and 250 as pulses for a photon energy of 58 eV. Normalizing the cross sections to that calculated for 1 fs helps display two important trends. First, at 10% energy sharing, which corresponds to one of the two equivalent sequential peaks in the SDCS, shorter pulses are accompanied by an increasingly back-to-back ejection pattern, very similar to that seen well

below the nonsequential threshold in Fig. 6. However for 50% energy sharing, away from the sequential peaks in the SDCS, the back-to-back pattern appears regardless of the pulse duration.

Thus it is the TDCS that reveals that different dynamics are being probed by pulses of different lengths. Subfemtosecond pulses show the signatures of the nonsequential mechanism of ejection at energy sharings where longer pulses show a very different angular pattern approximately described by the $\cos^2(\theta_1)\cos^2(\theta_2)$ angular distribution yielded by the approximate treatment given in the Appendix. In contrast to the TDCS, the behavior of the SDCS as the pulse duration is shortened can be described qualitatively and semiquantitatively by a simple approximation that includes only the effects of sequential ionization. Therefore, experiments seeking to establish how subfemtosecond pulses can probe the electron dynamics of photoejection will need to explore angular distributions associated with those pulses and not only the more integrated quantities of the SDCS and total cross sections.

It has come to our attention that similar results on the dependence of the SDCS and TDCS above the sequential threshold on pulse duration have been obtained by Feist *et al.* [30]. While their computed results are quite similar to the results we have obtained, their interpretation of those results is somewhat different from what we have presented.

Finally, we make some comments on the convergence of these results with respect to the inclusion of one-electron angular momenta and compare with some earlier calculations of the TDCS for double photoionization below the sequential threshold. In Fig. 9 we compare with the results of an earlier time-independent calculation, Horner *et al.* [20], and two time-dependent calculations, those of Hu *et al.* [31] and Feist *et al.* [21], for a photon energy of 42 eV. At energies so far below the sequential threshold, the TDCS extracted from finite duration pulses shows little dependence on the duration. Our calculations were performed with $l_{\max}=6$ and $T=550$ as. While the quantitative agreement is best with the recent studies of Feist *et al.*, there is qualitative agreement with the other studies, although the magnitudes differ by more than a factor of 2 in some cases.

We have observed that the convergence of the calculations with increasing l_{\max} is much faster when sequential ionization dominates, as one would expect because less final-state correlation is involved. Both the single and triple differential cross sections are practically converged with $l_{\max}=3$ in the sequential region. In the nonsequential region, a higher number of angular momenta must be included, regardless of the pulse duration, and angular momenta up to $l_{\max}=7$ must be included to converge the differential cross sections. Figure 10 compares the present calculations with the early time-dependent close-coupling (TDCC) results of Colgan and Pindzola [7] for a photon energy of 45 eV. We see that pulse durations on the order of 600 as or greater are sufficient to converge the TDCS at this energy and essentially complete convergence is achieved by $l_{\max}=7$. The differences between our calculations and the TDCC results are only significant for the TDCS in which one electron is fixed at 90° which is roughly 60 times smaller than at 0° .

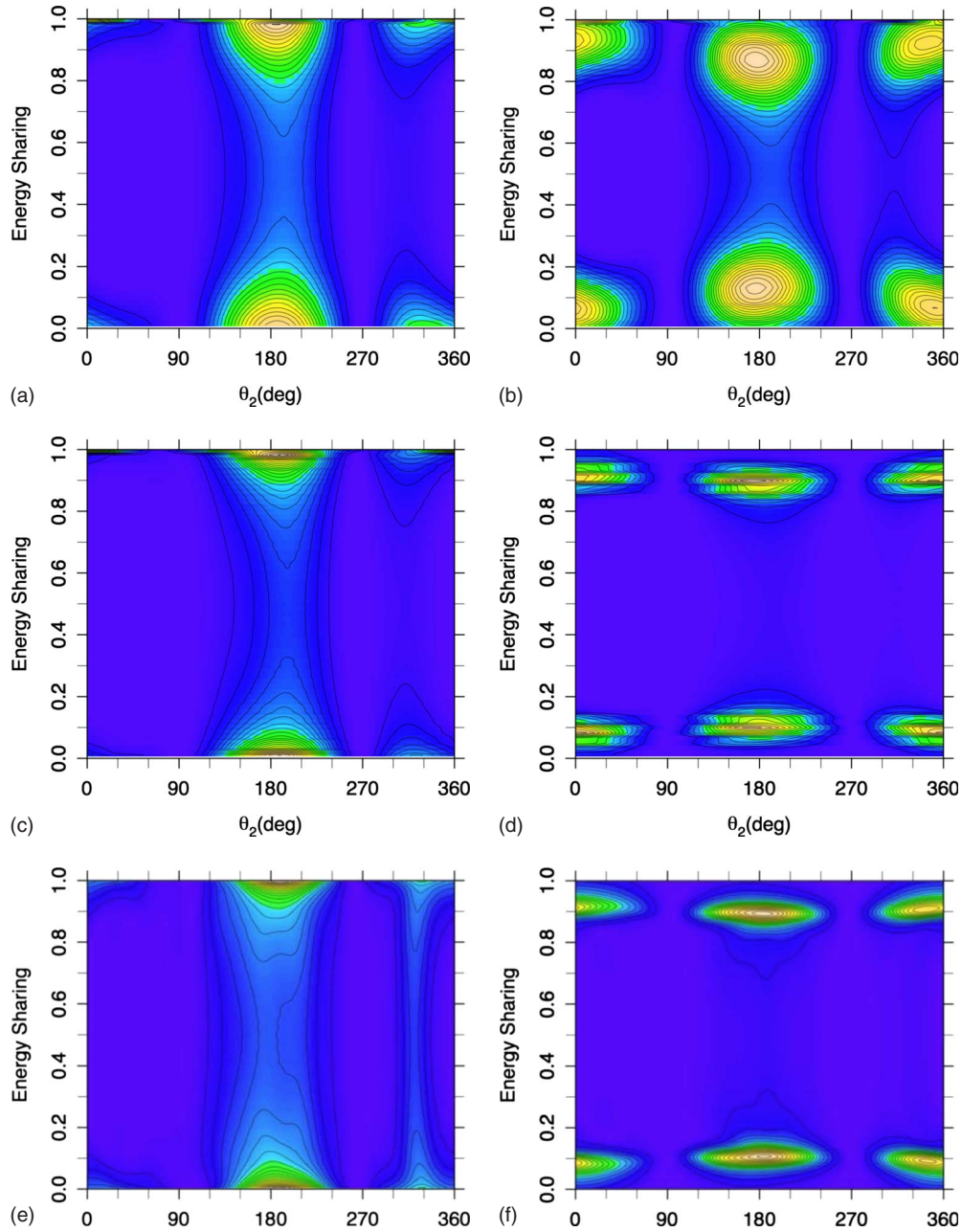


FIG. 7. (Color online) TDCS with one electron fixed at 0° from the polarization direction as a function of energy sharing. First row: 1 fs. Second row: 3 fs. Third row: results of Horner *et al.* [20]. Left column: 52 eV. Right column: 58 eV.

V. DOUBLE IONIZATION ABOVE THE SECOND SEQUENTIAL THRESHOLD

As the photon energy is raised further above the first sequential threshold we reach the threshold for sequential ionization in which the first step involves excitation ionization of the helium atom leaving the helium ion in its $2s$ or $2p$ state at 65.4 eV. At energies above this point, which we call the second sequential threshold, we expect to see four peaks in the SDCS at energies given by $E_1 = E_i - \epsilon_{1s} + \hbar\omega$, $E_1 = \epsilon_{1s} + \hbar\omega$, $E_1 = E_i - \epsilon_{2p} + \hbar\omega$, and $E_1 = \epsilon_{2p} + \hbar\omega$ since the $2p$ and $2s$ states of He^+ are degenerate. In Fig. 11 we scan the photon energy from 51.4 eV, below the first sequential threshold, to 70.0 eV, above the second sequential threshold. The SDCS

just below the first sequential threshold turns up at extreme energy sharings, as described previously [18], and for photon energies between the sequential thresholds the two peaks in the SDCS due to the sequential process involving the He^+ ion in its ground state appear and move toward equal-energy sharing.

At 70 eV we see the clear appearance of a second pair of peaks in the SDCS, with a smaller intensity expected because the cross section for excitation ionization is smaller than that for simple ionization of He. However closer inspection of that cross section yields a surprise. At 70 eV the second pair of sequential peaks should appear at 4.59 and 56.4 eV, respectively, but they appear shifted to higher and lower energies by nearly 2 eV. In Fig. 12 we plot the contri-

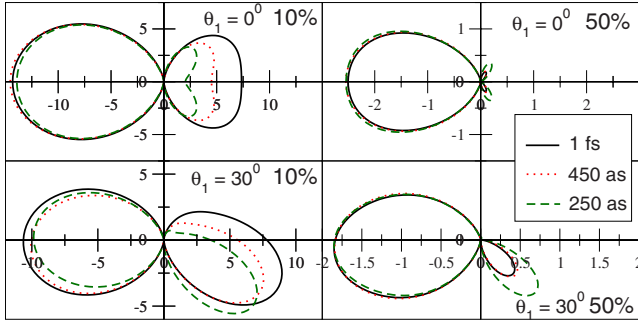


FIG. 8. (Color online) TDCS from calculations including up to $l_{\max}=7$ for a photon energy of 58 eV with energy sharing of 10% and 50% and pulse lengths of 1 fs, 450 as, and 250 as. Note that the all cross sections are normalized to the 1 fs TDCS for easier comparison of the shapes.

contributions of overall S and D symmetries to the SDCS at 70 eV and mark the expected energies of the sequential processes. It is apparent that the shift is present in both final symmetries.

For infinite-pulse durations, the sequential peaks in the SDCS always appear at the energies required by energy conservation. So this phenomenon must be related to the finite pulse lengths used here. To understand it qualitatively we can return to the simple approximations described in the Appendix. To generalize that treatment to energies above the second sequential threshold we must include contributions to Eq. (A3) due to the continuum states $\psi_{q,2s}$ and $\psi_{q,2p}$, which under the same approximations yield a version of Eq. (A7) with six terms in the square brackets. Those terms in the approximate sequential amplitude correspond to the ampli-

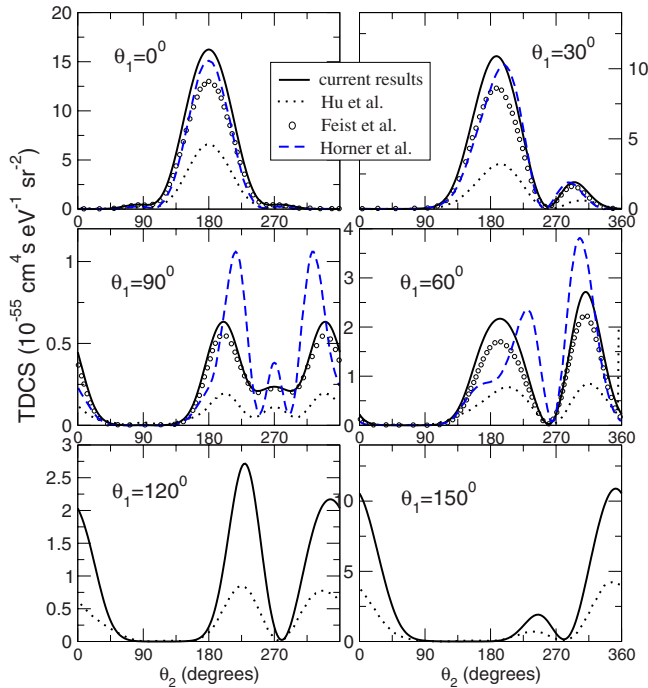


FIG. 9. (Color online) Comparison of the TDCS at 42 eV computed with $l_{\max}=6$ and $T=550$ as with the results of Refs. [20,31,21].

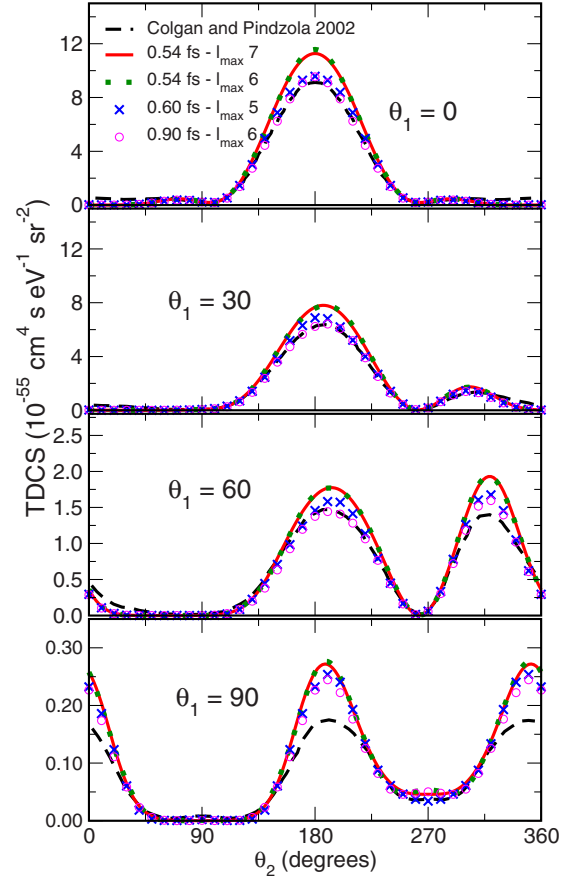


FIG. 10. (Color online) Calculated TDCS at 45 eV for various pulse durations and l_{\max} from 5 to 7 with comparisons to the TDCS results of Ref. [7].

tudes for ionization via the $1s$, $2s$, and $2p$ states of He^+ appearing as both direct and exchange terms. For finite pulses each such term contains a factor of $F(\alpha, T)$ that produces a finite peak height and width. However for pulses within our current computational abilities they remain broad enough to interfere with each other.

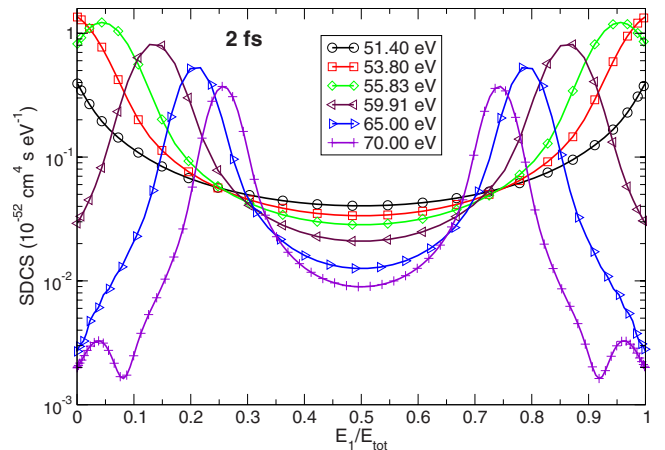


FIG. 11. (Color online) Calculated SDCS for pulse duration 2 fs for a range of photon energies from below the first sequential threshold to above the second sequential threshold.

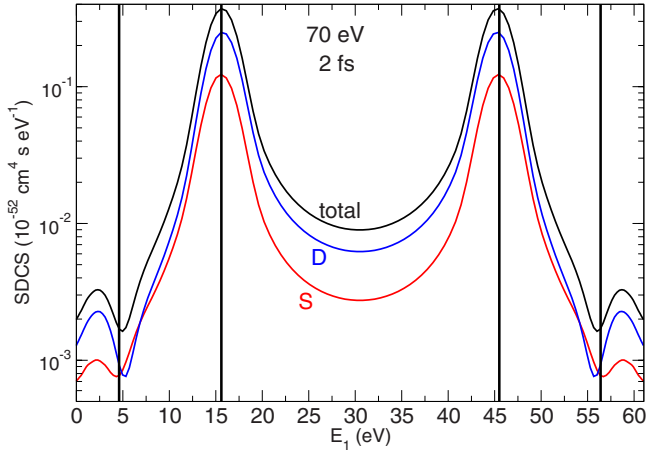


FIG. 12. (Color online) Calculated SDCS for pulse duration 2 fs at 70 eV showing the contributions of overall $1S$ and $1D$ symmetries and the shift in the peaks due to ionization via the $n=2$ states of He^+ .

Unfortunately, to model that interference from first principles we would need to retain the correct amplitudes in Eq. (A7) instead of neglecting their phases and relating them to the square roots of cross sections for the sequential processes. With assumed phases one can use such an approach to verify that an SDCS similar to that in Fig. 12 can be obtained, but we refrain from showing that result here, because it would amount to fitting the calculated cross section instead of approximating it from first principles as we have done with the SDCS between the sequential thresholds. We can conclude, however, that pulses longer than 2 or 3 fs will be required to see the sequential process producing peaks at the expected energies in the SDCS, and that, conversely, the effect in Fig. 12 is due exclusively to the pulse duration and does not require subfemtosecond pulses to be observed.

VI. CONCLUSION

We have demonstrated that a range of two-photon resonant single- and double-ionization processes can be calculated accurately by the methods developed in two previous publications [13,14] and applied here in large-scale calculations of the cross sections for both major and minor channels extracted from finite-length pulses. With the concept of an apparent cross section extracted from a pulse of duration T we can display the physics that can be resolved and probed by ultrashort pulses of durations $T \leq 3$ fs.

In the case of two-photon single ionization we have been able to see the appearance of the core excited resonances predicted by Shakeshaft and co-workers and thereby establish a time scale on which they disappear for very short pulses. In the case of two-photon double ionization we have explored the region above the first and second sequential thresholds and found dramatic dependences on T in the SDCS and TDCS for sequential double ionization proceeding via ionization of He to produce He^+ in its ground state and in its $n=2$ excited state.

The SDCS above the threshold for sequential ionization via the $1s$ state of He^+ varies dramatically with pulse length,

but a simple approximation including only the contribution of sequential ionization and requiring only a knowledge of the single-ionization cross section for each step reproduces that behavior. On the other hand, the variation with pulse duration of the TDCS for this process shows above that different electron dynamics are being probed in the subfemtosecond region than can be seen with pulses of durations of several femtoseconds.

The subtlety of the question of what dynamics is accessible in various kinds of measurements with different length pulses is emphasized by the last result we discussed here. While the pulse length dependence of the SDCS below the second sequential threshold is explainable using only sequential ionization cross sections and time-dependent perturbation theory, the SDCS above that threshold is not. It shows a signature of an interference effect between different sequential pathways that depends on the duration of the pulse used to ionize an atom.

ACKNOWLEDGMENTS

This work was performed under the auspices of the U.S. Department of Energy by the University of California Lawrence Berkeley National Laboratory under Contract No. DE-AC02-05CH11231 and was supported by the U.S. DOE Office of Basic Energy Sciences, Division of Chemical Sciences. C.W.M. acknowledges support from the National Science Foundation (Grant No. PHY-0604628).

APPENDIX: SIMPLE APPROXIMATION FOR SEQUENTIAL IONIZATION BY FINITE DURATION PULSE

To derive a simple approximation for the contribution of singly ionized state(s) of helium to double ionization we begin by retaining only the part of the interaction, $V_t = \mathbf{E}(t) \cdot \boldsymbol{\mu}$, due to the electric field in Eq. (2) that is associated with absorption (rotating wave approximation) from our \sin^2 pulse,

$$V_t = E_0 \mu \sin^2\left(\frac{\pi}{T} t\right) \frac{e^{i\omega t}}{2}, \quad (\text{A1})$$

where $\boldsymbol{\mu} = \boldsymbol{\mu}_1 + \boldsymbol{\mu}_2 = -ez_1 - ez_2$ is the electronic dipole operator. The formal expression from time-dependent perturbation theory for the amplitude for going from state i to state f in a two-photon transition is

$$\begin{aligned} C_{f \leftarrow i}^{(2)}(T) &= \left(\frac{-i}{\hbar}\right)^2 E_0^2 \sum_m \mu_{fm} \mu_{mi} \\ &\times \frac{1}{2} \int_0^T dt' e^{i(\omega_{fm} - \omega)t'} \sin^2(t' \pi/T) \\ &\times \frac{1}{2} \int_0^{t'} dt'' e^{i(\omega_{mi} - \omega)t''} \sin^2(t'' \pi/T), \quad (\text{A2}) \end{aligned}$$

where the sum over m is over bound and continuum intermediate states. Specializing this expression to the case of double ionization, and keeping only the intermediate states

corresponding to single ionization leaving the He^+ ion in its ground state, we obtain an approximation to the amplitude $C(\mathbf{k}_1, \mathbf{k}_2, T)$ of Eq. (6), which we now also label with the pulse duration T ,

$$\begin{aligned} C(\mathbf{k}_1, \mathbf{k}_2, T) &\approx \left(\frac{-i}{\hbar}\right)^2 E_0^2 \int d^3\mathbf{q} \langle \Psi_{\mathbf{k}_1\mathbf{k}_2}^- | \mu | \psi_{\mathbf{q},1s}^- \rangle \langle \psi_{\mathbf{q},1s}^- | \mu | \Phi_i \rangle \\ &\times \frac{1}{2} \int_0^T dt' e^{i[(E_1+E_2-E_q-\epsilon_{1s})/\hbar-\omega]t'} \sin^2(t' \pi/T) \\ &\times \frac{1}{2} \int_0^{t'} dt'' e^{i[(E_q+\epsilon_{1s}-E_i)/\hbar-\omega]t''} \sin^2(t'' \pi/T). \end{aligned} \quad (\text{A3})$$

In this expression $\Psi_{\mathbf{k}_1\mathbf{k}_2}^-$ is the final double-ionized-state wave function and $\psi_{\mathbf{q},1s}^-$ is the electron-ion scattering state corresponding to an electron of momentum \mathbf{q} incident on the He^+ ion in its ground state. The energies in the time integrals are $E_1 = \hbar^2 k_1^2 / 2m$, $E_2 = \hbar^2 k_2^2 / 2m$, $E_q = \hbar^2 q^2 / 2m$, and the energy of the He atom, E_i , in its ground state Φ_i .

The matrix element $\langle \psi_{\mathbf{q},1s}^- | \mu | \Phi_i \rangle$ can immediately be recognized as the amplitude for one-photon single ionization of He, but to proceed we need an approximation to the other amplitude in Eq. (A3),

$$\langle \Psi_{\mathbf{k}_1\mathbf{k}_2}^- | \mu | \psi_{\mathbf{q},1s}^- \rangle = \langle \Psi_{\mathbf{k}_1\mathbf{k}_2}^- | \mu_1 + \mu_2 | \psi_{\mathbf{q},1s}^- \rangle. \quad (\text{A4})$$

To approximate this matrix element we make the following two simplifying assumptions:

(1) Ignore final-state interaction completely so we can write the final state as a symmetrized product of Coulomb functions with charge $Z=2$,

$$\Psi_{\mathbf{k}_1\mathbf{k}_2}^- (\mathbf{r}_1, \mathbf{r}_2) \approx \mathcal{P} \{ \varphi_{\mathbf{k}_1}^{Z=2(-)} (\mathbf{r}_1) \varphi_{\mathbf{k}_2}^{Z=2(-)} (\mathbf{r}_2) \}, \quad (\text{A5})$$

where $\mathcal{P} = 1/\sqrt{2}(1+P_{12})$ is the symmetrizer (the intermediate states are all singlets) so that this wave function has delta-function normalization in momentum $[\delta(\mathbf{k}_1 - \mathbf{k}_1') \delta(\mathbf{k}_2 - \mathbf{k}_2')]$.

(2) Ignore any correlation in $\psi_{\mathbf{q},1s}^-$ and ignore screening of the outgoing electron by the $1s$ electron in He^+ , so that this wave function can be written as a product of a Coulomb function and the ground-state wave function of He^+ ,

$$\psi_{\mathbf{q},1s}^- \approx \varphi_{\mathbf{q}}^{Z=2(-)} (\mathbf{r}_1) \varphi_{1s}^{\text{He}^+} (\mathbf{r}_2). \quad (\text{A6})$$

With these approximations, the integral over $d^3\mathbf{q}$ in Eq. (A3) will be controlled by the delta function from the free-free overlap $\langle \varphi_{\mathbf{k}_1}^{Z=2(-)} | \varphi_{\mathbf{q}}^{Z=2(-)} \rangle = \delta(\mathbf{k}_1 - \mathbf{q})$ and we arrive at an approximation for the sequential ionization by a pulse of duration T in terms of the amplitudes for single ionization of He and He^+ ,

$$\begin{aligned} C(\mathbf{k}_1, \mathbf{k}_2, T) &\approx \left(\frac{-i}{\hbar}\right)^2 E_0^2 \frac{1}{\sqrt{2}} \\ &\times [\langle \varphi_{\mathbf{k}_2}^{Z=2(-)} | \mu | \varphi_{1s}^{\text{He}^+} \rangle \langle \psi_{\mathbf{k}_1,1s}^- | \mu | \Phi_0 \rangle F(\alpha_1, T) \\ &+ \langle \varphi_{\mathbf{k}_1}^{Z=2(-)} | \mu | \varphi_{1s}^{\text{He}^+} \rangle \langle \psi_{\mathbf{k}_2,1s}^- | \mu | \Phi_0 \rangle F(\alpha_2, T)]. \end{aligned} \quad (\text{A7})$$

The sum of the energies of the two outgoing electrons is now fixed by energy conservation as $E_1 + E_2 = E_i + 2\hbar\omega$, allowing the time integrals in Eq. (A3) to be simplified. They become the pulse-length-dependent factors $F(\alpha, T)$ with α equal to $\alpha_1 = (E_i + \hbar\omega - E_1 - \epsilon_{1s})/\hbar$ and $\alpha_2 = (E_i + \hbar\omega - E_2 - \epsilon_{1s})/\hbar$ and can be performed analytically to give a particularly simple result,

$$\begin{aligned} F(\alpha, T) &= \frac{1}{2} \int_0^T dt' e^{i\alpha t'} \sin^2(t' \pi/T) \frac{1}{2} \int_0^{t'} dt'' e^{-i\alpha t''} \sin^2(t'' \pi/T) \\ &= \frac{3iT^5 \alpha^5 - 20i\pi^2 T^3 \alpha^3 - 32\pi^4 (-iT\alpha + e^{iT\alpha} - 1)}{32(T^2 \alpha^3 - 4\pi^2 \alpha)^2}. \end{aligned} \quad (\text{A8})$$

Our expression for $C(\mathbf{k}_1, \mathbf{k}_2, T)$ in Eq. (A7) can be further approximated if we ignore the phases of the amplitudes and approximate the matrix elements in that equation using

$$\begin{aligned} \langle \psi_{\mathbf{k},1s}^- | \mu | \Phi_0 \rangle &\approx \left(\frac{\hbar}{(2\pi)^2 k \alpha \omega m} \frac{d\sigma}{d\Omega} \right)^{1/2} \\ &= \left(\frac{\hbar}{(2\pi)^2 k \alpha \omega m} \frac{\sigma^{\text{He}}(E)}{4\pi} \right. \\ &\quad \left. \times [1 + \beta^{\text{He}}(E) P_2(\cos(\theta))] \right)^{1/2} \end{aligned} \quad (\text{A9})$$

and with an analogous formula for the other amplitude, $\langle \varphi_{\mathbf{k}}^{Z=2(-)} | \boldsymbol{\epsilon} \cdot \mathbf{p} | \varphi_{1s}^{\text{He}^+} \rangle$. In the present case, both of these are simple s to p transitions, so $\beta=2$ and $1 + \beta P_2(\cos(\theta)) = 3 \cos^2(\theta)$.

With an approximation for the sequential contribution to $C(\mathbf{k}_1, \mathbf{k}_2, T)$ in hand the last step in extracting the apparent generalized cross section for two-photon ionization due to a pulse of duration T is to use Eq. (10). Evaluating $\tilde{\mathfrak{F}}(E_f, E_i, \omega, T)$ with $E_f = E_1 + E_2$ and at the peak of the shape function where $2\hbar\omega = E_1 + E_2 - E_i$ gives $\tilde{\mathfrak{F}} = 3iT/32$. Assembling the final result according to Eq. (10) we find the sequential contribution to the apparent TDCS for double ionization extracted from a pulse of duration T to be

$$\begin{aligned} \frac{d\sigma^{\text{seq}}(T)}{dE_1 d\Omega_1 d\Omega_2} &\approx \left(\frac{32}{3T}\right)^2 \frac{1}{4\pi\hbar} \left(\frac{3}{4\pi}\right)^2 \cos^2(\theta_1) \cos^2(\theta_2) \\ &\times \left| \sqrt{\sigma^{\text{He}^+}(E_2) \sigma^{\text{He}}(E_1) F(\alpha_1, T)} \right. \\ &\quad \left. + \sqrt{\sigma^{\text{He}^+}(E_1) \sigma^{\text{He}}(E_2) F(\alpha_2, T)} \right|^2. \end{aligned} \quad (\text{A10})$$

Equation (A10) has the characteristic $\cos^2(\theta_1)\cos^2(\theta_2)$ angular dependence of sequential ionization [18–20].

Integrating over the angles of the ejected electron gives the sequential contribution to the SDCS in this simple approximation,

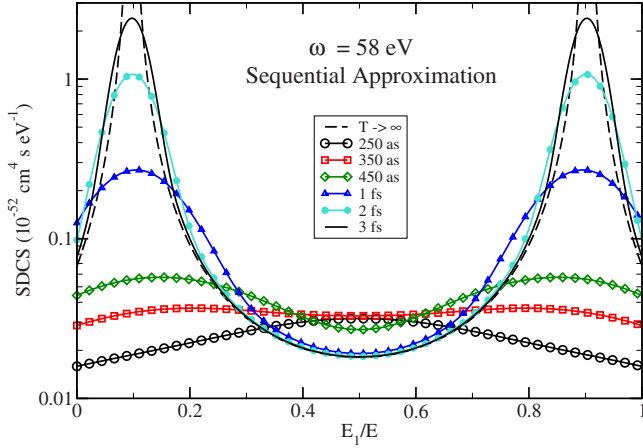


FIG. 13. (Color online) Simple sequential approximation from Eq. (A11) to the SDCS for various pulse durations for $\hbar\omega = 58$ eV.

$$\frac{d\sigma^{\text{seq}}(T)}{dE_1} \approx \left(\frac{32}{3T}\right)^2 \frac{1}{4\pi\hbar} \left| \sqrt{\sigma^{\text{He}^+}(E_2)\sigma^{\text{He}}(E_1)F(\alpha_1, T)} + \sqrt{\sigma^{\text{He}^+}(E_1)\sigma^{\text{He}}(E_2)F(\alpha_2, T)} \right|^2. \quad (\text{A11})$$

Using the well-known values of the cross sections for single ionization gives the SDCS shown in Fig. 13. Comparing this figure with Fig. 5 we see that this simple approximation to

the SDCS in the sequential region provides both the qualitative behavior with pulse duration and a remarkably good quantitative estimate of the accurately calculated SDCS in the sequential region. If at the outset in Eq. (A3) we had included intermediate singly ionized states of He^+ in the $2p$ and $2s$ states, four additional terms would have appeared in the final result instead of the two in Eq. (A7), each multiplied by the appropriate $F(\alpha, T)$ factor. However in that case the fact that the peaks are closer together makes it more important to include the correct phases of the amplitudes so that they can interfere properly.

Since $F(\alpha, T)$ peaks at $\alpha=0$ the factors $F(\alpha, T)$ produce peaks in the SDCS in Fig. 13 at the electron kinetic energies where the sequential process ejects electrons with $E_1=E_i - \epsilon_{1s} + \hbar\omega$ and $E_1=\epsilon_{1s} + \hbar\omega$, but only if the pulse duration is long enough. For pulses shorter than approximately 300 as the peaks do not appear at all and the maximum value of the apparent SDCS extracted from it is 2 orders of magnitude smaller than for a 3 fs pulse. In the long-time limit Eq. (A11) produces the simple approximation for the sequential contribution to the SDCS for an infinitely long pulse used previously [18–20],

$$\frac{d\sigma^{\text{seq}}}{dE_1} \approx \frac{\hbar}{4\pi} \left(\frac{\sqrt{\sigma^{\text{He}^+}(E_2)\sigma^{\text{He}}(E_1)}}{E_0 + \hbar\omega - \epsilon_{1s} - E_1} + \frac{\sqrt{\sigma^{\text{He}^+}(E_1)\sigma^{\text{He}}(E_2)}}{E_0 + \hbar\omega - \epsilon_{1s} - E_2} \right)^2 \quad (\text{A12})$$

in which the sequential peaks are singular.

- [1] P. Agostini and L. F. DiMauro, Rep. Prog. Phys. **67**, 813 (2004).
- [2] Th. Ergler, A. Rudenko, B. Feuerstein, K. Zrost, C. D. Schröter, R. Moshhammer, and J. Ullrich, Phys. Rev. Lett. **97**, 193001 (2006).
- [3] H. Niikura, D. M. Villeneuve, and P. B. Corkum, Phys. Rev. A **73**, 021402(R) (2006).
- [4] R. Kienberger *et al.*, Science **297**, 1144 (2002).
- [5] A. Scrinzi and B. Piraux, Phys. Rev. A **58**, 1310 (1998).
- [6] D. Dundas, K. T. Taylor, J. S. Parker, and E. S. Smyth, J. Phys. B **32**, L231 (1999).
- [7] J. Colgan and M. S. Pindzola, Phys. Rev. Lett. **88**, 173002 (2002).
- [8] K. T. Taylor, Phys. Scr., T **T105**, 31 (2003).
- [9] E. Fomouo, S. Laulan, B. Piraux, and H. Bachau, J. Phys. B **39**, S427 (2006).
- [10] I. F. Barna, J. Wang, and J. Burgdörfer, Phys. Rev. A **73**, 023402 (2006).
- [11] L. A. A. Nikolopoulos and P. Lambropoulos, J. Phys. B **40**, 1347 (2007).
- [12] M. S. Pindzola *et al.*, J. Phys. B **40**, R39 (2007).
- [13] A. Palacios, C. W. McCurdy, and T. N. Rescigno, Phys. Rev. A **76**, 043420 (2007).
- [14] A. Palacios, T. N. Rescigno, and C. W. McCurdy, Phys. Rev. A **77**, 032716 (2008).
- [15] T. N. Rescigno and C. W. McCurdy, Phys. Rev. A **62**, 032706 (2000).
- [16] D. Proulx, M. Pont, and R. Shakeshaft, Phys. Rev. A **49**, 1208 (1994).
- [17] R. Shakeshaft, Phys. Rev. A **76**, 063405 (2007).
- [18] D. A. Horner, F. Morales, T. N. Rescigno, F. Martín, and C. W. McCurdy, Phys. Rev. A **76**, 030701(R) (2007).
- [19] D. A. Horner, T. N. Rescigno, and C. W. McCurdy, Phys. Rev. A **77**, 030703(R) (2008).
- [20] D. A. Horner, C. W. McCurdy, and T. N. Rescigno, Phys. Rev. A **78**, 043416 (2008).
- [21] J. Feist, S. Nagele, R. Pazourek, E. Persson, B. I. Schneider, L. A. Collins, and J. Burgdörfer, Phys. Rev. A **77**, 043420 (2008).
- [22] C. W. McCurdy, M. Baertschy, and T. N. Rescigno, J. Phys. B **37**, R137 (2004).
- [23] A. Palacios, S. Barmaki, H. Bachau, and F. Martín, Phys. Rev. A **71**, 063405 (2005).
- [24] D. Charalambidis, D. Xenakis, C. Uiterwaal, P. Maragakis, J. Zhang, H. Shröder, O. Faucher, and P. Lambropoulos, J. Phys. B **30**, 1467 (1997).
- [25] S. Laulan and H. Bachau, Phys. Rev. A **68**, 013409 (2003).
- [26] L. Feng and H. W. van der Hart, J. Phys. B **36**, L1 (2003).
- [27] Y. K. Ho, Phys. Rep. **99**, 1 (1983).
- [28] H. Hasegawa, E. J. Takahashi, Y. Nabekawa, K. L. Ishikawa, and K. Midorikawa, Phys. Rev. A **71**, 023407 (2005).
- [29] A. A. Sorokin, M. Wellhöfer, S. V. Bobashev, K. Tiedtke, and M. Richter, Phys. Rev. A **75**, 051402(R) (2007).
- [30] J. Feist, S. Nagele, R. Pazourek, E. Persson, B. I. Schneider, L. A. Collins, and J. Burgdörfer, e-print arXiv:0901.4072.
- [31] S. X. Hu, J. Colgan, and L. A. Collins, J. Phys. B **38**, L35 (2005).